Theory and numerical evaluation of oddoids and evenoids: oscillatory cuspoid integrals with odd and even polynomial phase functions

C. A. Hobbs *

Department of Mathematical Sciences, School of Technology, Oxford Brookes University, Wheatley Campus, Oxford OX33 1HX, UK.

J.N.L. Connor *

School of Chemistry, The University of Manchester, Manchester M13 9PL, UK.

N. P. Kirk [1]

Department of Mathematical Sciences, University of Liverpool, Liverpool L69 3BX, UK.

Abstract

The properties of oscillating cuspoid integrals whose phase functions are odd and even polynomials are investigated. These integrals are called oddoids and evenoids respectively (and collectively, oddenoids). We have studied in detail oddenoids whose phase functions contain up to three real parameters. For each oddenoid, we have obtained its Maclaurin series representation and investigated its relation to Airy-Hardy integrals and Bessel functions of fractional orders. We have used techniques from singularity theory to characterise the caustic (or bifurcation set) associated with each oddenoid, including the occurrence of complex whiskers. Plots and short tables of numerical values for the oddenoids are presented. The numerical calculations used the software package CUSPINT [N P Kirk, J N L Connor and C A Hobbs, Comput. Phys. Commun. 132 (2000) 142–165].

Key words: Airy-Hardy integrals, Bessel functions of fractional order, Bifurcation set, Caustic, Complex whisker, CUSPINT, Cuspoid integrals, Evenoid integrals, Oddoid integrals, Oddenoid integrals, Oscillating integrals, Singularity theory, $\mathbf{Z}_2$-symmetry.

1 Introduction

This paper is the third in a series [29,30] concerned with the numerical evaluation and properties of oscillating integrals. In our first paper [29], we described a FORTRAN 90 code, called CUSPINT, which was written for the numerical computation by quadrature of the cuspoid canonical integrals

$$C_n(\alpha) = \int_{-\infty}^{\infty} \exp[\mathrm{i}(u^n + \sum_{j=1}^{n-2} \alpha_j u^j)]\mathrm{d}u, \qquad n = 3, 4, 5, ... \tag{1}$$

and their partial derivatives, where $\alpha = (\alpha_1, \alpha_2, ..., \alpha_{n-2})$ is a vector of real numbers.

CUSPINT implements a novel adaptive algorithm, which chooses contours in the complex u plane that avoid the violent oscillatory and exponential natures of the integrand and modifies its choice as necessary [29]. This adaptive contour algorithm has the advantage that it is relatively easy to implement on a computer, is efficient, and provides highly accurate results.

Our second paper [30] showed how a modified version of CUSPINT could be used for the numerical evaluation of other types of oscillating integrals; in particular we studied the bessoid canonical integral

$$J(x, y) = \int_0^{\infty} J_0(yu)u \exp[\mathrm{i}(u^4 + xu^2)]\mathrm{d}u \tag{2}$$

where $J_0(\bullet)$ denotes the Bessel function of order zero. The bessoid integral arises in the theory of axially symmetric cusped focusing [4,30,31,38,40, p.402]. In reference [19], two of us (CAH and JNLC) have provided an overview of the research reported in [29,30]. Gil et al. [22] have emphasised recently that quadrature methods are of great importance for the evaluation of special functions.

The purpose of this paper is to investigate the properties of two classes of oscillating integrals, which we will call *oddoids* and *evenoids*. The (real) oddoid integrals of order $k = 1, 2, 3, ...$ are defined by

* Corresponding authors.
Email addresses: cahobbs@brookes.ac.uk (C. A. Hobbs),
j.n.l.connor@manchester.ac.uk (J.N.L. Connor).
[1] Current address: Tenet Technology Ltd., North Heath Lane, Horsham, West Sussex, RH12 5UX, UK.

$$O_k(\mathbf{a}) = \int_{-\infty}^{\infty} \exp\left[\mathrm{i}\left(\frac{t^{2k+1}}{2k+1} + \sum_{j=1}^{k} a_j \frac{t^{2j-1}}{2j-1}\right)\right] \mathrm{d}t \tag{3}$$
$$= 2\int_{0}^{\infty} \cos\left(\frac{t^{2k+1}}{2k+1} + \sum_{j=1}^{k} a_j \frac{t^{2j-1}}{2j-1}\right) \mathrm{d}t$$

whereas the (complex) evenoid integrals of order $k = 1, 2, 3, ...$ are defined by

$$E_k(\mathbf{a}) = \int_{-\infty}^{\infty} \exp\left[\mathrm{i}\left(\frac{t^{2k+2}}{2k+2} + \sum_{j=1}^{k} a_j \frac{t^{2j}}{2j}\right)\right] \mathrm{d}t \tag{4}$$
$$= 2\int_{0}^{\infty} \exp\left[\mathrm{i}\left(\frac{t^{2k+2}}{2k+2} + \sum_{j=1}^{k} a_j \frac{t^{2j}}{2j}\right)\right] \mathrm{d}t$$

where $\mathbf{a} = (a_1, a_2, ..., a_k)$ is a vector of real numbers.

The "odd" and "even" parts of their names arise because the polynomial phases in the exponential functions of the integrals $O_k(\mathbf{a})$ and $E_k(\mathbf{a})$ are odd and even functions of t respectively, whereas the "oid" indicates their connection with the unfolding of a cuspoid singularity. When we need to refer to both classes of integrals, we will use the noun *oddenoids* (not to be confused with adenoids).

Although $O_k(\mathbf{a})$ and $E_k(\mathbf{a})$ are special cases of the cuspoid canonical integral (see Section 2.1), it is often convenient to consider them as forming separate classes of canonical integral, because the odd-ness or even-ness of their integrand phases is usually enforced by symmetry in practical applications.

We will be particularly concerned with cases where the orders of $O_k(\mathbf{a})$ and $E_k(\mathbf{a})$ have the values $k = 1, 2$ and 3, since it is very difficult to visualise integrals depending on more than three real parameters.

1.1 Oddenoids of order $k = 1$

The definition (3) shows that the first oddoid integral

$$O_1(a_1) = \int_{-\infty}^{\infty} \exp\left[\mathrm{i}\left(\frac{t^3}{3} + a_1 t\right)\right] \mathrm{d}t = 2\pi Ai(a_1) \tag{5}$$

is proportional to the regular Airy function, $Ai(a_1)$ – also sometimes called the *fold* canonical integral when the terminology of elementary catastrophe

theory [43,51] is used for the phase of the integrand. The properties and many applications of the Airy function are well known [1,39,47], and $O_1(a_1)$ is only briefly considered in this paper.

The leading evenoid integral is obtained from the definition (4)

$$E_1(a_1) = \int_{-\infty}^{\infty} \exp\left[\mathrm{i}\left(\frac{t^4}{4} + a_1\frac{t^2}{2}\right)\right] \mathrm{d}t \tag{6}$$

which shows that $E_1(a_1)$ is related to the Pearcey integral (or *cusp* canonical integral [51]), $C_4(\alpha_1, \alpha_2)$, as a special case. The integral (6) arises in the theory of cusped focusing [2,5,9,10,12–14,21,27,40,41].

1.2 Oddenoids of order $k = 2$

The oddoid integral of order two is given by

$$O_2(a_1, a_2) = \int_{-\infty}^{\infty} \exp\left[\mathrm{i}\left(\frac{t^5}{5} + a_2\frac{t^3}{3} + a_1 t\right)\right] \mathrm{d}t \tag{7}$$

It is a special case of the *swallowtail* canonical integral [51], $C_5(\alpha_1, \alpha_2, \alpha_3)$. The integral (7) arises in the semiclassical theory of bound-continuum Franck-Condon factors [17,32] and in the theory of scattering processes in intense laser fields [33,34].

The corresponding evenoid integral is

$$E_2(a_1, a_2) = \int_{-\infty}^{\infty} \exp\left[\mathrm{i}\left(\frac{t^6}{6} + a_2\frac{t^4}{4} + a_1\frac{t^2}{2}\right)\right] \mathrm{d}t \tag{8}$$

which is a special case of the *butterfly* canonical integral [51], $C_6(\alpha_1, \alpha_2, \alpha_3, \alpha_4)$. Main [36] and Fabčič et al. [20] have shown that this integral arisies in the semiclassical theory of quantum spectra.

1.3 Oddenoids of order $k = 3$

The definition (3) shows that this oddoid integral has the representation

$$O_3(a_1,a_2,a_3)=\int_{-\infty}^{\infty}\exp\left[\mathrm{i}\left(\frac{t^7}{7}+a_3\frac{t^5}{5}+a_2\frac{t^3}{3}+a_1t\right)\right]\mathrm{d}t \tag{9}$$

which is a special case of the *wigwam* canonical integral, $C_7(\alpha_1,\alpha_2,\alpha_3,\alpha_4,\alpha_5)$ [51].

Finally, the evenoid integral of order three is given by

$$E_3(a_1,a_2,a_3)=\int_{-\infty}^{\infty}\exp\left[\mathrm{i}\left(\frac{t^8}{8}+a_3\frac{t^6}{6}+a_2\frac{t^4}{4}+a_1\frac{t^2}{2}\right)\right]\mathrm{d}t \tag{10}$$

It is a special case of the *star* canonical integral [51], $C_8(\alpha_1,\alpha_2,\alpha_3,\alpha_4,\alpha_5,\alpha_6)$. The integrals (9) and (10) arise in general theories of short wavelength scattering, eg. [10,11,18,28,37].

Note: All the integrals (1)–(10) are conditionally convergent. Also, we do not consider oddenoid integrals of order zero, since O_0 is proportional to a Dirac delta function of unit argument

$$O_0=\int_{-\infty}^{\infty}\exp(\mathrm{i}t)\mathrm{d}t=2\pi\delta(1)$$

and the evenoid integral of order zero can be explicitly evaluated

$$E_0=\int_{-\infty}^{\infty}\exp\left(\mathrm{i}t^2/2\right)\mathrm{d}t=(2\pi)^{1/2}\exp(\mathrm{i}\pi/4)$$

In section 2, we derive some useful properties of the oddenoids for $k=1,2,3$, in particular their Maclaurin series expansions. We also show how the oddenoids, for special values of their parameters, can be related to Airy-Hardy integrals and hence to Bessel functions of fractional orders. Section 3 derives the (non-standard) caustics associated with the oddenoids using techniques from singularity theory. We show that each oddoid and evenoid of the same order has the same caustic. Our analysis allows for the coalescence of both real- and complex-valued critical points, the latter giving rise to complex whiskers. In section 4, we report plots and short tables of numerical values for oddenoids with $k=1,2,3$, computed using CUSPINT. Our concluding remarks are in section 5.

2 Properties of $O_k(\mathbf{a})$ and $E_k(\mathbf{a})$

This section derives some properties of the oddenoids that are useful for their numerical evaluation.

2.1 Relation of the oddenoids to the cuspoid canonical integrals

The $O_k(\mathbf{a})$ and $E_k(\mathbf{a})$ are special cases of the cuspoid oscillatory integral defined by equation (1). The $C_n(\alpha)$ have been studied in refs [8,11,16,18,29], where many references to earlier research can be found.

To obtain the oddenoids, we first make the change of variable $u = t/n^{1/n}$ in the integral (1). This gives

$$C_n(\alpha) = \frac{1}{n^{1/n}} \int_{-\infty}^{\infty} \exp\left[\mathrm{i}\left(\frac{t^n}{n} + \sum_{j=1}^{n-2} \alpha_j \frac{t^j}{n^{j/n}}\right)\right] \mathrm{d}t \tag{11}$$

We then proceed as follows:

(a) To obtain the $O_k(\mathbf{a})$ (where $n = 2k+1$), multiply equation (11) by $n^{1/n}$, set all the α_{2j} for $j = 1, 2, ..., (n-3)/2$, to zero and put

$$\alpha_{2j-1} = \frac{n^{(2j-1)/n}}{2j-1} a_j, \qquad j = 1, 2, ..., k$$

(b) To obtain the $E_k(\mathbf{a})$ (where $n = 2k+2$), multiply equation (11) by $n^{1/n}$, set all the α_{2j-1} for $j = 1, 2, ..., (n-2)/2$, to zero and put

$$\alpha_{2j} = \frac{n^{2j/n}}{2j} a_j, \qquad j = 1, 2, ..., k$$

2.2 Maclaurin series expansions for the oddenoids

The Maclaurin series for $O_k(\mathbf{a})$ and $E_k(\mathbf{a})$, for specific values of k, can be derived from the Maclaurin series for $C_n(\alpha)$. This series has been given for arbitrary n in [10]. The technique used in [10] is to write $C_n(\alpha)$ as the sum of two semi-infinite integrals. Then the two rays from 0 to ∞ are replaced by two rays in the complex u plane, with the help of Cauchy's theorem and Jordan's Lemma, thereby producing two absolutely convergent integrals. The exponential integrands are next expanded in multiple power series, the summation and

integration signs can be safely interchanged and the resulting Maclaurin series expressed in terms of gamma functions, $\Gamma(\bullet)$ [46].

All the Maclaurin series given below converge for all values of $a_1, a_2, ...$; they provide an alternative way to compute numerically the oddenoids. Previously such series representations were most useful for small $|a_1|$, $|a_2|, ...$, because of cancellation and slow convergence when the computations were performed using single or double precision arithmetic. However, the availability of arbitrary precision software means that Maclaurin series are now a useful computational tool for a wider range of parameter values.

From equations (4.1)–(4.10) of [10] and the manipulations described in Section 2.1, we obtain the following Maclaurin series for the oddenoids after simplification.

2.2.1 Oddenoids of order $k = 1$

$$O_1(a_1) = \frac{2}{3^{2/3}} \sum_{n=0}^{\infty} \frac{a_1^n}{n!} 3^{n/3} \Gamma\left(\frac{1+n}{3}\right) \cos\left(\frac{\pi}{6}(1+4n)\right) \tag{12}$$

Dividing the series (12) by 2π gives us a standard series representation [47, p.11, equation (2.26)] for $Ai(a_1)$ – see also equation (5).

$$E_1(a_1) = \frac{1}{2^{1/2}} \sum_{n=0}^{\infty} \frac{a_1^n}{n!} \Gamma\left(\frac{1+2n}{4}\right) \exp\left(\frac{\mathrm{i}\pi}{8}(1+6n)\right) \tag{13}$$

2.2.2 Oddenoids of order $k = 2$

$$O_2(a_1, a_2) = \frac{2}{5^{4/5}} \sum_{n=0}^{\infty} \sum_{m=0}^{\infty} \frac{a_1^n}{n!} \frac{a_2^m}{m!} \frac{5^{(n+3m)/5}}{3^m} \Gamma\left(\frac{1+n+3m}{5}\right) \times \cos\left(\frac{\pi}{10}(1+6n+8m)\right) \tag{14}$$

$$E_2(a_1, a_2) = \frac{6^{1/6}}{3} \sum_{n=0}^{\infty} \sum_{m=0}^{\infty} \frac{a_1^n}{n!} \frac{a_2^m}{m!} \frac{3^{(n+2m)/3}}{2^{(2n+4m)/3}} \Gamma\left(\frac{1+2n+4m}{6}\right) \times \exp\left(\frac{\mathrm{i}\pi}{12}(1+8n+10m)\right) \tag{15}$$

2.2.3 Oddenoids of order $k = 3$

$$O_3(a_1, a_2, a_3) = \frac{2}{7^{6/7}} \sum_{n=0}^{\infty} \sum_{m=0}^{\infty} \sum_{p=0}^{\infty} \frac{a_1^n}{n!} \frac{a_2^m}{m!} \frac{a_3^p}{p!} \frac{7^{(n+3m+5p)/7}}{3^m 5^p} \Gamma\left(\frac{1+n+3m+5p}{7}\right) \times \cos\left(\frac{\pi}{14}(1+8n+10m+12p)\right) \quad (16)$$

$$E_3(a_1, a_2, a_3) = \frac{1}{2^{13/8}} \sum_{n=0}^{\infty} \sum_{m=0}^{\infty} \sum_{p=0}^{\infty} \frac{a_1^n}{n!} \frac{a_2^m}{m!} \frac{a_3^p}{p!} \frac{1}{2^{(n+2m-5p)/4} 3^p} \Gamma\left(\frac{1+2n+4m+6p}{8}\right) \times \exp\left(\frac{\mathrm{i}\pi}{16}(1+10n+12m+14p)\right) \quad (17)$$

Note: an oddenoid of order k has a k-tuple series representation.

2.3 Value of the oddenoids at the origin

We can evaluate the oddenoids at the origin, $\mathbf{a} = \mathbf{0}$, with the help of the result [24,45]

$$\int_0^{\infty} \exp(\pm \mathrm{i} u^n)\, \mathrm{d}u = \frac{1}{n} \Gamma\left(\frac{1}{n}\right) \exp\left(\pm \mathrm{i} \frac{\pi}{2n}\right), \qquad n = 2, 3, 4, ... \quad (18)$$

We then obtain from the definitions (3) and (4)

$$O_k(\mathbf{0}) = \frac{2}{(2k+1)^{2k/(2k+1)}} \Gamma\left(\frac{1}{2k+1}\right) \cos\left[\frac{\pi}{2(2k+1)}\right] \quad (19)$$

and

$$E_k(\mathbf{0}) = \frac{2}{(2k+2)^{(2k+1)/(2k+2)}} \Gamma\left(\frac{1}{2k+2}\right) \exp\left[\mathrm{i} \frac{\pi}{2(2k+2)}\right] \quad (20)$$

As a check on equations (19) and (20), we note that they reduce to the leading terms of the Maclaurin series (12) – (17) for $k = 1, 2, 3$.

The oddenoids, for special values of their parameters, can be related to Airy-Hardy integrals, which in turn can be expressed in terms of Bessel functions of fractional orders [25,48,47, Chap. 6.1]. This provides an alternative numerical procedure for the evaluation of the oddenoids in this special case.

We first need the following results given by Watson [48]. Define for positive or negative $a(\neq 0)$

$$T_n(t,a) = t^n {}_2F_1\left(-\frac{1}{2}n, \frac{1}{2} - \frac{1}{2}n; 1-n; -\frac{4a}{t^2}\right) \qquad a \neq 0$$

Evaluation of the hypergeometric function for $n = 3, 4, ..., 8$ results in

$$\left.\begin{aligned} T_3(t,a) &= t^3 + 3at \\ T_4(t,a) &= t^4 + 4at^2 + 2a^2 \\ T_5(t,a) &= t^5 + 4at^3 + 5a^2t \\ T_6(t,a) &= t^6 + 6at^4 + 9a^2t^2 + 2a^3 \\ T_7(t,a) &= t^7 + 7at^5 + 14a^2t^3 + 7a^3t \\ T_8(t,a) &= t^8 + 8at^6 + 20a^2t^4 + 16a^3t^2 + 2a^4 \end{aligned}\right\} \tag{21}$$

It can be seen that the polynomials in equation (21) are special cases of the integrand phases for the oddenoids, as described in section 1. Airy-Hardy integrals have the $T_n(t,a)$ as their integrand phases and can be evaluated in terms of Bessel functions of fractional orders [48]. We will consider the cases $n = 2p+1$ and $n = 2p$, for p a positive integer, separately.

(a) The case $n = 3, 5, 7, ...$

The Airy-Hardy cosine integral for $n = 2p+1$, where p is a positive integer, is given by [48]

$$\begin{aligned} Ch_n(a) &\equiv \int_0^\infty \cos\left[T_n(t,a)\right] \mathrm{d}t \\ &= \frac{\pi |a|^{1/2}}{2n \sin(\pi/2n)} \times \begin{cases} I_{-\frac{1}{n}}\left(2a^{n/2}\right) - I_{\frac{1}{n}}\left(2a^{n/2}\right) & a > 0 \\ J_{-\frac{1}{n}}\left(2|a|^{n/2}\right) + J_{\frac{1}{n}}\left(2|a|^{n/2}\right) & a < 0 \end{cases} \end{aligned} \tag{22}$$

where $J_\nu(x)$ is a Bessel function of the first kind and $I_\nu(x)$ is a modified Bessel

function of the first kind.

(b) The case $n = 4, 6, 8, ...$

Watson [48] has derived the following results for the Airy-Hardy cosine and sine integrals when $n = 2p$ for p a positive integer (N.B. valid for both $a > 0$ and $a < 0$),

$$Ch_n(a) = \frac{\pi|a|^{1/2}}{2n\sin(\pi/2n)}\left[J_{-\frac{1}{n}}\left(2|a|^{n/2}\right) - \mathrm{sign}(a)J_{\frac{1}{n}}\left(2|a|^{n/2}\right)\right] \tag{23}$$

and

$$\begin{aligned} Sh_n(a) &\equiv \int_0^\infty \sin\left[T_n(t,a)\right]\mathrm{d}t \\ &= \frac{\pi|a|^{1/2}}{2n\cos(\pi/2n)}\left[J_{-\frac{1}{n}}\left(2|a|^{n/2}\right) + \mathrm{sign}(a)J_{\frac{1}{n}}\left(2|a|^{n/2}\right)\right] \end{aligned} \tag{24}$$

from which it follows that

$$\begin{aligned} Eh_n(a) &\equiv \int_0^\infty \exp\left[\mathrm{i}T_n(t,a)\right]\mathrm{d}t \\ &= \frac{\pi|a|^{1/2}}{2n\sin(\pi/n)}\left[e^{\mathrm{i}\pi/2n}J_{-\frac{1}{n}}\left(2|a|^{n/2}\right) + \mathrm{sign}(a)e^{-\mathrm{i}\pi/2n}J_{\frac{1}{n}}\left(2|a|^{n/2}\right)\right] \end{aligned} \tag{25}$$

Note: equations (22)–(25) in the limit $a \to 0$ become special cases of equation (18), upon using the following results for $n = 3, 4, 5, ...$

$$\begin{aligned} \lim_{x\to 0} x^{1/2}J_{-\frac{1}{n}}\left(2x^{n/2}\right) &= \lim_{x\to 0} x^{1/2}I_{-\frac{1}{n}}\left(2x^{n/2}\right) = \frac{1}{\pi}\Gamma\left(\frac{1}{n}\right)\sin\left(\frac{\pi}{n}\right) \\ \lim_{x\to 0} x^{1/2}J_{\frac{1}{n}}\left(2x^{n/2}\right) &= \lim_{x\to 0} x^{1/2}I_{\frac{1}{n}}\left(2x^{n/2}\right) = 0 \end{aligned}$$

We now use equations (22) and (25), together with the change of variables described in section 2.1, to evaluate the oddenoids for $k = 1, 2, 3$ in terms of Bessel functions.

2.4.1 *Oddenoids of order $k = 1$*

Equation (22) expresses $O_1(a)$ in terms of Bessel functions of order $\pm 1/3$, which is simply related to a well-known result for the regular Airy integral, since $O_1(a) = 2\pi Ai(a)$ (see [47], p.20, equations (2.79) and (2.80)).

For the $k = 1$ evenoid, we obtain from equation (25)

$$E_1(a) = \frac{1}{2}\pi|a|^{1/2}\exp\left(-\mathrm{i}a^2/8\right)\left[e^{\mathrm{i}\pi/8}J_{-\frac{1}{4}}\left(a^2/8\right) - \mathrm{sign}(a)e^{-\mathrm{i}\pi/8}J_{\frac{1}{4}}\left(a^2/8\right)\right] \tag{26}$$

$E_1(a)$ can also be written [13] in terms of a parabolic cylinder function, $D_\nu(z)$, of order $-1/2$, namely

$$E_1(a) = 2^{1/4}\pi^{1/2}\exp\left(-\mathrm{i}\frac{1}{8}a^2 + \mathrm{i}\frac{1}{8}\pi\right)D_{-\frac{1}{2}}\left(\frac{e^{-\mathrm{i}\pi/4}a}{2^{1/2}}\right) \tag{27}$$

where $D_{-\frac{1}{2}}(z)$ has the integral representation

$$D_{-\frac{1}{2}}(z) = \frac{\exp\left(-\frac{1}{4}z^2\right)}{\pi^{1/2}}\int_0^\infty \exp\left(-\frac{1}{2}s^2 - zs\right)s^{-1/2}\mathrm{d}s \tag{28}$$

which is a special case of [35, p.328].

$$D_\nu(z) = \frac{\exp\left(-\frac{1}{4}z^2\right)}{\Gamma(-\nu)}\int_0^\infty \exp\left(-\frac{1}{2}s^2 - zs\right)s^{-\nu-1}\mathrm{d}s \quad \mathrm{Re}(\nu) < 0$$

Equations (26)–(28) provide two alternative schemes for the numerical computation of $E_1(a)$. One by evaluation of Bessel functions of orders $\pm 1/4$ [12,13]; the other by quadrature of the integral (28).

2.4.2 *Oddenoids of order $k = 2$*

Equations (22) and (25) respectively yield

$$O_2\left(\frac{a^2}{9}, a\right) = \frac{\pi|a|^{1/2}}{3^{1/2}5\sin(\pi/10)} \times \begin{cases} I_{-\frac{1}{5}}\left(\frac{2a^{5/2}}{3^{1/2}45}\right) - I_{\frac{1}{5}}\left(\frac{2a^{5/2}}{3^{1/2}45}\right) & a > 0 \\ J_{-\frac{1}{5}}\left(\frac{2|a|^{5/2}}{3^{1/2}45}\right) + J_{\frac{1}{5}}\left(\frac{2|a|^{5/2}}{3^{1/2}45}\right) & a < 0 \end{cases} \tag{29}$$

and

$$E_2\left(\frac{3}{16}a^2, a\right) = \frac{1}{3}\pi|a|^{1/2}\exp\left(\frac{-\mathrm{i}a^3}{192}\right)\left[e^{\mathrm{i}\pi/12}J_{-\frac{1}{6}}\left(\frac{|a|^3}{192}\right) - \mathrm{sign}(a)e^{-\mathrm{i}\pi/12}J_{\frac{1}{6}}\left(\frac{|a|^3}{192}\right)\right] \quad (30)$$

2.4.3 Oddenoids of order $k = 3$

We obtain for $k = 3$ the results

$$O_3\left(\frac{a^3}{125}, \frac{6a^2}{25}, a\right) = \frac{\pi|a|^{1/2}}{5^{1/2}7\sin(\pi/14)} \times \begin{cases} I_{-\frac{1}{7}}\left(\frac{2a^{7/2}}{5^{1/2}875}\right) - I_{\frac{1}{7}}\left(\frac{2a^{7/2}}{5^{1/2}875}\right) & a > 0 \\ J_{-\frac{1}{7}}\left(\frac{2|a|^{7/2}}{5^{1/2}875}\right) + J_{\frac{1}{7}}\left(\frac{2|a|^{7/2}}{5^{1/2}875}\right) & a < 0 \end{cases} \quad (31)$$

and

$$E_3\left(\frac{a^3}{54}, \frac{5a^2}{18}, a\right) = \frac{\pi|a|^{1/2}\exp\left(-\mathrm{i}a^4/5184\right)}{6^{1/2}4\sin(\pi/8)}\left[e^{\mathrm{i}\pi/16}J_{-\frac{1}{8}}\left(\frac{a^4}{5184}\right) - \mathrm{sign}(a)e^{-\mathrm{i}\pi/16}J_{\frac{1}{8}}\left(\frac{a^4}{5184}\right)\right] \quad (32)$$

It can be checked that, in the limit $a \to 0$, equations (26), (29)–(32) reduce to the formulae reported in section 2.3 for the oddenoids evaluated at $\mathbf{a} = \mathbf{0}$. In addition, for the parabolic cylinder function representation (27) of $E_1(a)$, we can use [35, p.324].

$$D_\nu(0) = \frac{\Gamma(\frac{1}{2})2^{\nu/2}}{\Gamma((1-\nu)/2)} \quad (33)$$

with $\nu = -1/2$ to obtain $E_1(0)$.

2.5 Differential equations for the oddenoids

$O_1(a_1)$ satisfies the same linear differential equation as the regular Airy function, since $O_1(a_1) = 2\pi Ai(a_1)$. We have therefore

$$\frac{\mathrm{d}^2 O_1(a_1)}{\mathrm{d}a_1^2} = a_1 O_1(a_1) \tag{34}$$

Thus another numerical method (see e.g., [15]) for evaluating $O_1(a_1)$ would be to integrate equation (34) from $a_1 = 0$ to the value of a_1 of interest, using the Maclaurin series representation (12) to find the initial conditions, $O_1(0)$ and $O_1'(0)$, where the prime indicates differentiation with respect to a_1.

In [16] it has been shown that this method can be generalised, i.e., a set of differential equations can be written down satisfied by the $C_n(\alpha_1, \alpha_2, ..., \alpha_{n-2})$, using the Maclaurin series to give initial conditions. In particular, this approach has been used to evaluate the Pearcey [12,13,15,26] and swallowtail [15] canonical integrals, $C_4(y, x)$ and $C_5(z, y, x)$, respectively. For the oddenoids, it is clear that the differential equations they satisfy can be derived from the cuspoid equations as special cases. However, we do not derive the oddenoid differential equations here (except for $E_1(a_1)$), since we have not used this approach to compute numerical values in the present paper.

The reasons we *do* derive the differential equation for $E_1(a_1)$ are (a) it is easily obtained from the theory of Airy-Hardy integrals, already presented in section 2.4, and (b) a useful identity for $E_1(a_1)$ can be readily deduced from the differential equation. In the remainder of this section, we will write a rather than a_1 for notational simplicity.

From section 2.4, the relation between the evenoid, $E_1(a)$, and the Airy-Hardy integral $Eh_4(a)$, is

$$E_1(a) = 2^{1/2} \exp\left(-\frac{\mathrm{i}a^2}{8}\right) Eh_4\left(\frac{a}{4}\right) \tag{35}$$

Now, it is known [48] that for $n = 4, 6, 8, ...$, both $Ch_n(a)$ and $Sh_n(a)$ (and hence also $Eh_n(a)$) are annihilated by the differential operator $\mathrm{d}^2/\mathrm{d}a^2 + n^2 a^{n-2}$. Hence, $Eh_4(a/4)$, which we will temporarily write as $\psi(a)$, obeys

$$\frac{\mathrm{d}^2 \psi(a)}{\mathrm{d}a^2} + \frac{a^2}{16}\psi(a) = 0 \tag{36}$$

Next we change the dependent variable in equation (36) from $\psi(a)$ to $E_1(a)$ using equation (35), to obtain

$$\frac{\mathrm{d}^2 E_1(a)}{\mathrm{d}a^2} + \frac{\mathrm{i}a}{2}\frac{\mathrm{d}E_1(a)}{\mathrm{d}a} + \frac{\mathrm{i}}{4}E_1(a) = 0 \tag{37}$$

Equation (37) is the linear differential equation satisfied by the $k = 1$ evenoid.

Equation (36) will be recognised as a Schrödinger equation for a parabolic potential energy barrier, with the total energy equal to the barrier maximum. We now calculate the flux associated with this Schrödinger equation, which will yield a useful identity for $E_1(a)$ and its first derivative.

First we multiply equation (36) by $\psi^*(a)$ giving

$$\psi^*(a)\frac{\mathrm{d}^2\psi(a)}{\mathrm{d}a^2} + \frac{a^2}{16}\psi^*(a)\psi(a) = 0 \tag{38}$$

Second we subtract from equation (38) its complex conjugate, which leads to

$$\psi(a)\frac{\mathrm{d}^2\psi^*(a)}{\mathrm{d}a^2} - \psi^*(a)\frac{\mathrm{d}^2\psi(a)}{\mathrm{d}a^2} = 0 \tag{39}$$

or equivalently

$$\frac{\mathrm{d}}{\mathrm{d}a}\left[\psi(a)\frac{\mathrm{d}\psi^*(a)}{\mathrm{d}a} - \psi^*(a)\frac{\mathrm{d}\psi(a)}{\mathrm{d}a}\right] = 0$$

which on integration gives the result

$$\psi(a)\frac{\mathrm{d}\psi^*(a)}{\mathrm{d}a} - \psi^*(a)\frac{\mathrm{d}\psi(a)}{\mathrm{d}a} = \text{constant} \tag{40}$$

Third we use equation (35) to change from $\psi(a) \equiv Eh_4(a/4)$ to $E_1(a)$ in equation (40) obtaining

$$\mathrm{Im}\left[\left(\frac{\mathrm{d}E_1(a)}{\mathrm{d}a} + \frac{\mathrm{i}a}{4}\right)^* E_1(a)\right] = \text{constant} \tag{41}$$

Now, the identity (41) is true for all values of a. We can determine the constant by evaluating the lhs at $a = 0$ with the help of the Maclaurin series representation for $E_1(a)$. From the Maclaurin series (13), we find $E_1(0) = \Gamma(1/4)\exp(\mathrm{i}\pi/8)/2^{1/2}$ and $E_1'(0) = \Gamma(3/4)\exp(\mathrm{i}7\pi/8)/2^{1/2}$. Hence, after simplification, the constant is found to be $-\pi/2$. Equation (41) then becomes

$$\mathrm{Im}\left[\left(\frac{\mathrm{d}E_1(a)}{\mathrm{d}a} + \frac{\mathrm{i}a}{4}\right)^* E_1(a)\right] = -\frac{\pi}{2} \tag{42}$$

Equation (42) is an identity satisfied by $E_1(a)$ and its first derivative. It provides a useful check on any numerical method used to compute these quantities. Finally, we note that the derivation of the identity (42) given above using Airy-Hardy integrals is completely different from that in [15] for the analogous identity obeyed by $C_4(y = 0, x)$.

3 Properties of the caustics for $O_k(\mathbf{a})$ and $E_k(\mathbf{a})$

In this section we shall use techniques from singularity theory to derive results for the *caustics* (or *bifurcation sets*) of $O_k(\mathbf{a})$ and $E_k(\mathbf{a})$. We then examine the cases $k = 1, 2, 3$ in more detail. Caustics play an important role in understanding structure in oscillating integrals such as the $O_k(\mathbf{a})$ and $E_k(\mathbf{a})$ [11,28,37,42,44,50]. For general notation and basic results from singularity theory we refer to [6].

3.1 Some concepts from singularity theory

The phase functions of the evenoids can be written in the form $f(u^2)$ for some function germ $f : \mathbf{K}, 0 \to \mathbf{K}, 0$ (where $\mathbf{K}$ denotes $\mathbf{R}$ or $\mathbf{C}$ as appropriate). Similarly, functions consisting entirely of odd powers of u can be written in the form $uf(u^2)$ for some function germ $f : \mathbf{K}, 0 \to \mathbf{K}, 0$. Such odd functions are known as functions with $\mathbf{Z}_2$-symmetry [23, Chap. 6].

Note: A *function germ* is an equivalence class of functions, where two functions are said to be equivalent if they are equal on a neighbourhood of the origin. This allows us to concentrate on behaviour around the origin without being distracted by behaviour further away. We can take any member of the equivalence class to be a representative of that function germ, and in general think of their representatives just like functions, but with the proviso that we are only considering their local behaviour. From now on we will refer to *functions* where strictly we should write *function germs*, as is usual in the literature [6].

The set of all functions of the form $f(u^2)$ is a *ring*, denoted $\mathcal{O}_{u^2}$. Note that a ring of functions is a set of functions which is closed under addition and multiplication, obeys the usual rules of algebra for addition and multiplication, has a zero element and additive inverses in the set. In the present case we are just interested in the fact that the set of functions consisting of even powers of u is closed under addition and multiplication by other functions which consist of even powers of u.

The set of all functions of the form $uf(u^2)$, denoted by $u\mathcal{O}_{u^2}$, is a *module*

over the ring $\mathcal{O}_{u^2}$ [23, Chap. 6]. A module over a ring is a set which is closed under addition and under scalar multiplication, where the scalars come from the ring. In this case, the module is the set of all functions consisting of odd powers of u, which is clearly closed under addition and under multiplication by functions of the type $f(u^2)$.

We can now use standard classification results (see Chapter 3 of [6]) to classify $\mathcal{O}_{u^2}$ and $p.324$ up to $\mathcal{R}$-equivalence.

Note: Functions $f, g \in \mathcal{O}_{u^2}$ (respectively, $uf, ug \in u\mathcal{O}_{u^2}$) are *$\mathcal{R}$-equivalent* if there exists a diffeomorphism $\phi : \mathbf{K}, 0 \to \mathbf{K}, 0$ such that $f(u^2) = g(\phi(u)^2)$ (respectively, $uf(u^2) = \phi(u)g(\phi(u)^2)$). That is, we consider two functions to be equivalent if a smooth change of co-ordinates in the variable u can change one into the other.

Using the standard classification results [6], in the even case we get the *normal form* as u^{2k+2} for $k \geq 0$, with *miniversal unfolding* in $\mathcal{O}_{u^2}$ given by

$$F^e(u, \mathbf{a}) = u^{2k+2} + a_k u^{2k} + \cdots + a_2 u^4 + a_1 u^2 \tag{43}$$

and in the odd case the normal form is u^{2k+1} for $k \geq 0$, with miniversal unfolding in $u\mathcal{O}_{u^2}$ given by

$$F^o(u, \mathbf{a}) = u^{2k+1} + a_k u^{2k-1} + \cdots + a_2 u^3 + a_1 u \tag{44}$$

Note: An *unfolding* of a function f is a family of functions containing f. Certain unfoldings contain *all* functions close to f (in a precise sense – see Chapter 6 of [6]), and we call these *versal* unfoldings. A versal unfolding with the minimum number of parameters needed to contain all functions close to f is called *miniversal*.

3.2 Properties of the caustic

We would like to understand the caustic, or bifurcation set, of $F(u, \mathbf{a})$, (where F denotes F^e or F^o as appropriate) given by

$$\mathrm{Bif}_{\mathbf{R}} F = \{\mathbf{a} \in \mathbf{R}^k : \exists u \in \mathbf{R} \text{ with } F_u(u, \mathbf{a}) = F_{uu}(u, \mathbf{a}) = 0\} \tag{45}$$

where the subscripts represent partial differentiation with respect to u. The roots of the first equation, $F_u(u, \mathbf{a}) = 0$, defines the (real or complex) *critical points*, and the second equation, $F_{uu}(u, \mathbf{a}) = 0$, is the condition that two or

more critical points are equal. $\mathrm{Bif}_{\mathbf{R}} F$ is defined by eliminating u from the two equations, subject to u being real. $\mathrm{Bif}_{\mathbf{R}} F$ may be different from

$$\mathrm{Bif}\, F = \{\mathbf{a} \in \mathbf{R}^k : \exists u \in \mathbf{C} \text{ with } F_u(u, \mathbf{a}) = F_{uu}(u, \mathbf{a}) = 0\} \tag{46}$$

which allows for two or more *complex* critical points to be equal. $\mathrm{Bif}\, F$ may be easier to calculate than $\mathrm{Bif}_{\mathbf{R}} F$; clearly $\mathrm{Bif}_{\mathbf{R}} F \subseteq \mathrm{Bif}\, F$.

Remark: Poston and Stewart, in Chapter 4 of [42], denote as *complex whiskers* those parts of $\mathrm{Bif}\, F$ coming from repeated complex critical points. In general, complex whiskers are sets of higher codimension than the rest of the hypersurface $\mathrm{Bif}\, F$, as being a repeated complex root of $F_u(u, \mathbf{a}) = 0$ imposes further conditions on their real and imaginary parts (since complex roots must necessarily appear in complex conjugate pairs for real $\mathbf{a}$). However, in our examples we have functions F with a high symmetry, which forces their bifurcation sets to be of higher codimension than one might generally expect for a polynomial of degree $2k+1$ or $2k+2$. We find that the subsets of $\mathrm{Bif}\, F$ corresponding to real and complex repeated roots have the same codimension for our examples.

We will study the bifurcation sets for the even and odd cases by relating the unfoldings (43) and (44) to a certain function, denoted $G(z, \mathbf{a})$, whose bifurcation set is already known. First we rescale the miniversal unfoldings (43) and (44) to be consistent with the polynomial phases in the integrals (4) and (3) respectively.

$$F^e(u, \mathbf{a}) = \frac{u^{2k+2}}{2k+2} + a_k \frac{u^{2k}}{2k} + \cdots + a_2 \frac{u^4}{4} + a_1 \frac{u^2}{2} \tag{47}$$

$$F^o(u, \mathbf{a}) = \frac{u^{2k+1}}{2k+1} + a_k \frac{u^{2k-1}}{2k-1} + \cdots + a_2 \frac{u^3}{3} + a_1 u \tag{48}$$

Now consider the function

$$G(z, \mathbf{a}) = \frac{z^{k+1}}{k+1} + a_k \frac{z^k}{k} + \ldots + a_2 \frac{z^2}{2} + a_1 z \tag{49}$$

This is a versal unfolding of an A_k singularity (see Chapter 6 of [6]), but is not a miniversal unfolding as it includes the term $a_k z^k/k$, and $G(z, \mathbf{a})$ contains the same k parameters $a_1, a_2, \ldots, a_k$ as do $F^e(u, \mathbf{a})$ and $F^o(u, \mathbf{a})$.

Notice that in the even case, $F^e_u(u, \mathbf{a}) = uG_z(u^2, \mathbf{a})$ (where we set $z = u^2$ after differentiation) and so $F^e_{uu}(u, \mathbf{a}) = 2u^2 G_{zz}(u^2, \mathbf{a}) + G_z(u^2, \mathbf{a})$, whereas in the odd case, $F^o_u(u, \mathbf{a}) = G_z(u^2, \mathbf{a})$ and $F^o_{uu} = 2uG_{zz}(u^2, \mathbf{a})$, so the bifurcation sets

of $F^e(u, \mathbf{a})$ and $F^o(u, \mathbf{a})$ are related to the bifurcation set of $G(z, \mathbf{a})$. More precisely, we have the following theorem.

Theorem 3.1*(i)* $\mathrm{Bif}\, F = \mathrm{Bif}_1\, F \cup \mathrm{Bif}_2\, F \subset \mathbf{R}^k$
(ii) $\mathrm{Bif}_{\mathbf{R}}\, F = \mathrm{Bif}_1\, F \cup \mathrm{Bif}_3\, F \subset \mathbf{R}^k$

where $\mathrm{Bif}_1\, F = \{(a_1, a_2, ..., a_k) \in \mathbf{R}^k : a_1 = 0\}$, $\mathrm{Bif}_2\, F = \mathrm{Bif}\, G$ *and*

$\mathrm{Bif}_3\, F = \{\mathbf{a} \in \mathrm{Bif}_{\mathbf{R}}\, G$ *with corresponding coalesced critical point* $z \geq 0\}$.

Proof In the even case, the defining equations for the bifurcation set are

$$F^e_u(u, \mathbf{a}) = uG_z(u^2, \mathbf{a}) = 0 \tag{50}$$

and

$$F^e_{uu}(u, \mathbf{a}) = 2u^2 G_{zz}(u^2, \mathbf{a}) + G_z(u^2, \mathbf{a}) = 0 \tag{51}$$

whereas in the odd case, the defining equations are

$$F^o_u(u, \mathbf{a}) = G_z(u^2, \mathbf{a}) = 0 \tag{52}$$

and

$$F^o_{uu}(u, \mathbf{a}) = 2uG_{zz}(u^2, \mathbf{a}) = 0 \tag{53}$$

In both cases, *either* $u = 0$ and $G_z(0, \mathbf{a}) = 0$, *or* $G_{zz}(z, \mathbf{a}) = G_z(z, \mathbf{a}) = 0$. In the first situation we see that $a_1 = 0$, upon differentiation of equation (49), yielding the hyperplane $\{(a_1, a_2, ..., a_k) \in \mathbf{R}^k : a_1 = 0\}$. In the second case, by definition of the bifurcation set, we obtain $\mathrm{Bif}\, G$ upon elimination of z, or $\mathrm{Bif}_{\mathbf{R}}\, G$ if we restrict to $z \in \mathbf{R}$. Note: for $\mathrm{Bif}_{\mathbf{R}}\, G$, u will only be real if $z \geq 0$ since $u = z^{1/2}$. Also note that $\mathrm{Bif}\, G$ is empty for $k = 1$. □

This theorem is useful as we already have descriptions of $\mathrm{Bif}\, G$ from standard results in singularity theory. Since $G(z, \mathbf{a})$ is a versal unfolding of $z^{k+1}/(k+1)$ with k parameters, it is equivalent to the constant unfolding (i.e. with one parameter) of the standard $k-1$ parameter miniversal unfolding of $z^{k+1}/(k+1)$. Two equivalent unfoldings with the same number of parameters have diffeomorphic bifurcation sets, so $\mathrm{Bif}\, G$ will be diffeomorphic to the Cartesian product of the standard bifurcation set of $z^{k+1}/(k+1)$ with $\mathbf{R}$. However, this does not necessarily help us understand how the hyperplane $\{(a_1, a_2, ..., a_k) \in$

$\mathbf{R}^k : a_1 = 0\}$ (which, for simplicity, we will henceforth write as $\{a_1 = 0\}$) and $\mathrm{Bif}\, G$ are arranged in $\mathbf{R}^k$ for $k > 1$. We now prove the following:

Theorem 3.2 *For $k > 1$, the two components of* $\mathrm{Bif}\, F$ *intersect tangentially.*

Proof We have $\mathrm{Bif}_1 F = \{a_1 = 0\}$, which (trivially) has tangent plane $\{a_1 = 0\}$.

Now $\mathrm{Bif}_2 F$ is in general singular at the origin, $\mathbf{a} = \mathbf{0}$, so consider the *tangent cone* at the origin. For a hypersurface defined by the equation $f = 0$, the tangent cone is given by the vanishing of the non-zero homogeneous component of f of smallest total degree (see Chapter 9, Section 7 of [7]). The hypersurface $\mathrm{Bif}_2 F = \{G_z(z, \mathbf{a}) = G_{zz}(z, \mathbf{a}) = 0\}$ is equivalently defined using the resultant, $f = \mathrm{Res}(G_z(z, \mathbf{a}), G_{zz}(z, \mathbf{a}), z) = 0$. Now for $k > 1$

$$\mathrm{Res}(G_z(z, \mathbf{a}), G_{zz}(z, \mathbf{a}), z) = k^k a_1^{k-1} + O(a_i^k), \quad i = 1, ..., k \tag{54}$$

This can be seen by considering the resultant as the determinant of the $(2k - 1) \times (2k - 1)$ Sylvester matrix of $G_z(z, \mathbf{a})$ and $G_{zz}(z, \mathbf{a})$ and noting that the terms of smallest total degree in the determinant of this matrix are those expanded about the maximum possible number of non-zero numerical entries of the matrix. This maximum is obtained by expanding about the k entries appearing on the diagonal of the bottom left $k \times k$ submatrix, which are all the number k. The remaining part of this term in the determinant comes from the top right $(k - 1) \times (k - 1)$ submatrix which is lower triangular with a_1 down the main diagonal.

The result (54) shows that the non-zero homogeneous component of smallest total degree is proportional to a_1^{k-1}, so the tangent cone of $\mathrm{Bif}_2 F$ is $a_1^{k-1} = 0$ and is thus also given by $\{a_1 = 0\}$. Therefore the two components of the bifurcation set, $\mathrm{Bif}_1 F$ and $\mathrm{Bif}_2 F$, are tangential. □

In summary, our approach is to define the appropriate $G(z, \mathbf{a})$ for a given phase function $F(u, \mathbf{a})$ (with all even or all odd power terms), then to find the bifurcation set of $G(z, \mathbf{a})$ and finally to relate it to the bifurcation set of $F(u, \mathbf{a})$ using Theorems 3.1 and 3.2.

3.3 Bifurcation sets for oddenoids of orders $k = 1, 2, 3$

3.3.1 Oddenoids of order $k = 1$

$E_1(a_1)$ has the phase function

$$F^e(u, a_1) = \frac{u^4}{4} + a_1 \frac{u^2}{2}$$

and that for $O_1(a_1)$ is

$$F^o(u, a_1) = \frac{u^3}{3} + a_1 u$$

The corresponding $G(z, a_1)$ is

$$G(z, a_1) = \frac{z^2}{2} + a_1 z$$

Now $G_z(z, a_1) = 0$ only has a single root, so $\mathrm{Bif}\, G$ and $\mathrm{Bif}_{\mathbf{R}}\, G$ are empty. Then by Theorem 3.1, $F^e(u, a_1)$ and $F^o(u, a_1)$ have a repeated root if and only if $a_1 = 0$. Of course, this result that $\mathrm{Bif}\, F = \mathrm{Bif}_{\mathbf{R}}\, F = \{a_1 = 0\}$ for $F(u, a_1) = F^e(u, a_1)$ or $F^o(u, a_1)$ is easily checked by direct analysis of their phase functions.

3.3.2 Oddenoids of order $k = 2$

The phase function for $E_2(a_1, a_2)$ is

$$F^e(u, a_1, a_2) = \frac{u^6}{6} + a_2 \frac{u^4}{4} + a_1 \frac{u^2}{2}$$

whilst that for $O_2(a_1, a_2)$ is given by

$$F^o(u, a_1, a_2) = \frac{u^5}{5} + a_2 \frac{u^3}{3} + a_1 u$$

Hence the corresponding $G(z, a_1, a_2)$ is

$$G(z, a_1, a_2) = \frac{z^3}{3} + a_2 \frac{z^2}{2} + a_1 z \tag{55}$$

In both cases, $\mathrm{Bif}_1\, F = \{a_1 = 0\}$ and $\mathrm{Bif}_2\, F = \mathrm{Bif}\, G$. We can calculate $\mathrm{Bif}\, G$ by eliminating z from $G_z(z, a_1, a_2) = G_{zz}(z, a_1, a_2) = 0$, i.e. eliminating z from $z^2 + a_2 z + a_1 = 0$ and $2z + a_2 = 0$, which yields $a_1 = a_2^2/4$. The full bifurcation set

$$\operatorname{Bif} F = \{a_1 = 0\} \cup \{a_1 = a_2^2/4\}$$

is shown in figure 1. (Note: the resultant $\operatorname{Res}(G_z(z, a_1, a_2), G_{zz}(z, a_1, a_2), z)$ is $4a_1 - a_2^2$ in agreement with equation (54) for $k = 2$). We observe that the condition $2z + a_2 = 0$ forces z to be real, since a_2 is real by definition, so in fact $\operatorname{Bif} G = \operatorname{Bif}_{\mathbf{R}} G$ in this case.

But we showed in Section 3.1 that $(a_1, a_2) \in \operatorname{Bif}_{\mathbf{R}} F$ only if $z \geq 0$, which means that $\operatorname{Bif}_{\mathbf{R}} F$ corresponds to $a_2 \leq 0$ in $\operatorname{Bif}_{\mathbf{R}} G$. Thus we have

$$\operatorname{Bif}_{\mathbf{R}} F = \{a_1 = 0\} \cup \{a_1 = a_2^2/4 : a_2 \leq 0\}$$

This semi-algebraic set is plotted in figure 2.

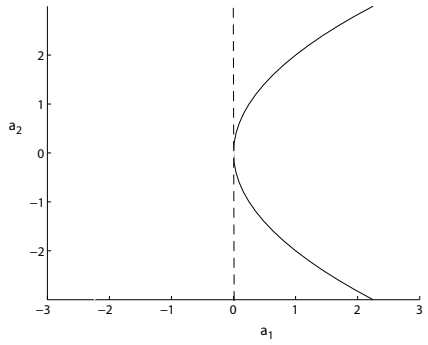

Fig. 1. $\operatorname{Bif} F$ for $E_2(a_1, a_2)$ and $O_2(a_1, a_2)$ where $F(u, a_1, a_2) = F^e(u, a_1, a_2)$ or $F^o(u, a_1, a_2)$. The dashed line is $a_1 = 0$.

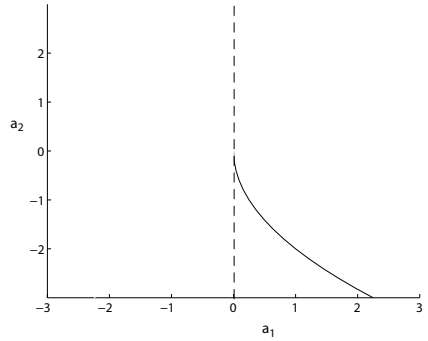

Fig. 2. $\operatorname{Bif}_{\mathbf{R}} F$ for $E_2(a_1, a_2)$ and $O_2(a_1, a_2)$ where $F(u, a_1, a_2) = F^e(u, a_1, a_2)$ or $F^o(u, a_1, a_2)$. The dashed line is $a_1 = 0$.

It is worth noting that we can derive the same results by working parametrically. In order to solve $z^2 + a_2 z + a_1 = 0$ and $2z + a_2 = 0$, we see that $a_2 = -2z$ and so $a_1 = z^2$. Thus $\operatorname{Bif}_{\mathbf{R}} G = \{(z^2, -2z) : z \in \mathbf{R}\}$. For $\operatorname{Bif}_{\mathbf{R}} F$, we must have $z \geq 0$, so

$$\mathrm{Bif}_{\mathbf{R}}\, F = \{a_1 = 0\} \cup \{(z^2, -2z) : z \geq 0\}$$

3.3.3 Oddenoids of order $k = 3$

$E_3(a_1, a_2, a_3)$ has phase function

$$F^e(u, a_1, a_2, a_3) = \frac{u^8}{8} + a_3\frac{u^6}{6} + a_2\frac{u^4}{4} + a_1\frac{u^2}{2}$$

with the phase function for $O_3(a_1, a_2, a_3)$ being

$$F^o(u, a_1, a_2, a_3) = \frac{u^7}{7} + a_3\frac{u^5}{5} + a_2\frac{u^3}{3} + a_1 u$$

The corresponding $G(z, a_1, a_2, a_3)$ is

$$G(z, a_1, a_2, a_3) = \frac{z^4}{4} + a_3\frac{z^3}{3} + a_2\frac{z^2}{2} + a_1 z$$

Then $\mathrm{Bif}_1 F = \{a_1 = 0\}$ and $\mathrm{Bif}_2 F = \mathrm{Bif}\, G$. To find $\mathrm{Bif}\, G$ we must eliminate z from the equations

$$G_z(z, a_1, a_2, a_3) = z^3 + a_3 z^2 + a_2 z + a_1 = 0 \tag{56}$$
$$G_{zz}(z, a_1, a_2, a_3) = 3z^2 + 2a_3 z + a_2 = 0 \tag{57}$$

Using Maple 9.5 to eliminate z from equations (56) and (57), we obtain

$$27a_1^2 - 18a_1a_2a_3 - a_2^2a_3^2 + 4a_1a_3^3 + 4a_2^3 = 0 \tag{58}$$

The variety defined by equation (58) is a twisted cuspidal edge which meets the plane $a_1 = 0$ in $a_2^2(a_3^2 - 4a_2) = 0$.

Note: the resultant $\mathrm{Res}(G_z(z, a_1, a_2, a_3), G_{zz}(z, a_1, a_2, a_3), z)$ is the lhs of equation (58), and agrees with equation (54) for $k = 3$. Again we observe that $G_z(z, a_1, a_2, a_3) = 0$ has no repeated complex roots (in this case because $G_z(z, a_1, a_2, a_3)$ is a cubic in z, and we would need $G_z(z, a_1, a_2, a_3)$ to be of at least degree 4 in z in order to have repeated complex roots, which necessarily come in complex conjugate pairs for real a_1, a_2, a_3). So $\mathrm{Bif}\, G = \mathrm{Bif}_{\mathbf{R}}\, G$ again. We then have

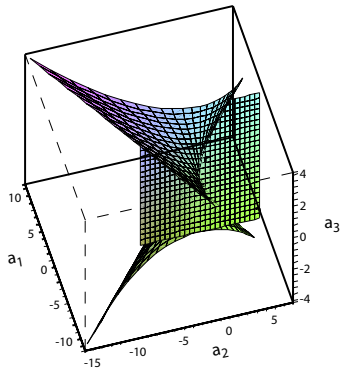

Fig. 3. Bif F for $E_3(a_1, a_2, a_3)$ and $O_3(a_1, a_2, a_3)$ where $F(u, a_1, a_2, a_3) = F^e(u, a_1, a_2, a_3)$ or $F^o(u, a_1, a_2, a_3)$. The plane is $a_1 = 0$.

$$\text{Bif}\, F = \{a_1 = 0\} \cup \{27a_1^2 - 18a_1a_2a_3 - a_2^2a_3^2 + 4a_1a_3^3 + 4a_2^3 = 0\}$$

which is plotted in figure 3. The twisted cuspidal edge and tangential plane can be clearly seen.

To find $\text{Bif}_{\mathbf{R}}\, F$, we use the parametric approach since we need to restrict the variety (58) to $z \geq 0$. Equations (57) and (56) give $a_2 = -3z^2 - 2a_3z$ and $a_1 = 2z^3 + a_3z^2$ respectively, so the surface $\text{Bif}_{\mathbf{R}}\, G$ is given parametrically by $\text{Bif}_{\mathbf{R}}\, G = \{(2z^3 + yz^2, -3z^2 - 2yz, y) : y, z \in \mathbf{R}\}$. To get $\text{Bif}_{\mathbf{R}}\, F$ we need $z \geq 0$. Thus we have

$$\text{Bif}_{\mathbf{R}}\, F = \{a_1 = 0\} \cup \{(2z^3 + yz^2, -3z^2 - 2yz, y) : y, z \in \mathbf{R}, z \geq 0\} \qquad (59)$$

Figure 4 shows that the semi-algebraic set $\text{Bif}_{\mathbf{R}}\, F$ is a 'half-cuspidal edge' plus the tangential plane.

We also note that our calculations of Bif F and $\text{Bif}_{\mathbf{R}}\, F$ for $F = F^o(u, a_1, a_2, a_3)$ are relevant to Problem 1992-4 in the book *Arnold's Problems* [3].

4 Numerical results for $O_k(\mathbf{a})$ and $E_k(\mathbf{a})$ of orders $k = 1, 2, 3$

In this section, we evaluate the oddenoids numerically. We have used the adaptive contour code, CUSPINT, outlined in Section 1, which we have applied to the oddenoids following the prescriptions of Section 2.1.

We show plots of the $O_k(\mathbf{a})$ and $E_k(\mathbf{a})$ for $k = 1, 2, 3$ (with the exception of

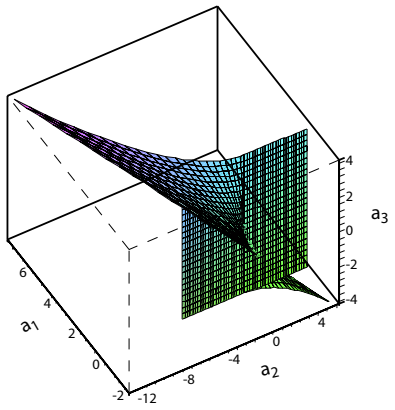

Fig. 4. $\mathrm{Bif}_{\mathbf{R}} F$ for $E_3(a_1, a_2, a_3)$ and $O_3(a_1, a_2, a_3)$ where $F(u, a_1, a_2, a_3) = F^e(u, a_1, a_2, a_3)$ or $F^o(u, a_1, a_2, a_3)$. The plane is $a_1 = 0$.

$O_1(a_1)$). Recall from Section 1 that the $O_k(\mathbf{a})$ are purely real, whereas the $E_k(\mathbf{a})$ are complex valued, so in this case we plot the modulus of $E_k(\mathbf{a})$. Our computer program can be used to calculate numerical values of the oddenoids for $k > 3$, but we do not do this here because the results are less easy to visualise.

For each plot, we also display the corresponding caustic obtained by elimination of u subject to u being real from the defining equation (45). Each caustic acts as a "skeleton" upon which is built the "wave flesh" of the corresponding oddenoid. In addition, we have added to the caustic diagrams the number of real critical points in each connected region of parameter space. In general we expect the richest structure in the oddenoid plots to occur in the regions with the largest number of real critical points. This is because there is a contribution from each real critical point when the simple stationary phase method [49] is used to evaluate an oscillating integral; their contributions then interfere to produce structure in an oddenoid. As we cross the caustic we expect an oddenoid to take large, but finite, values, rather than being infinite as predicted by the simple stationary phase method [49].

Following previous practice [29,30], we also report a short table of numerical values for each oddenoid (except for $O_1(a_1)$). The tabulated values are provided merely as test data so that readers can check the output from their own computer programs – our code can easily evaluate thousands of numerical values for each integral. This is what has been done to generate the plots, but tables of such size would be impractical to reproduce here.

For each oddenoid, the tabulated values have been checked using Maple 9.5 to evaluate the integrals by summation of the Maclaurin series given in Section 2.2. Agreement, to as many significant figures as required, can be obtained by increasing the number of terms in the Maclaurin series. Note that Maple 9.5 is significantly slower at performing the evaluations for our tables than

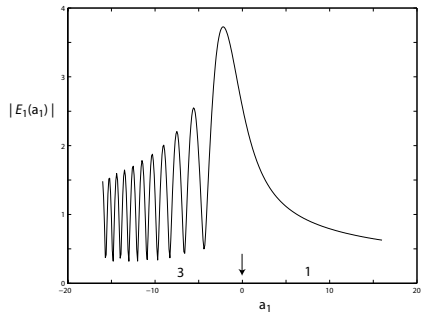

Fig. 5. Plot of $|E_1(a_1)|$ for the grid $a_1 = -16.0(0.001)16.0$. The arrow indicates the caustic at $a_1 = 0$

is CUSPINT. For example, the calculations in Table 4 took over 3 days using Maple 9.5 on an Intel 3.4 GHz machine with 2 Gb memory to reach the same accuracy as CUSPINT achieved in a matter of seconds on a similar machine.

4.1 Oddenoids of order $k = 1$

The oddoid of order 1, $O_1(a_1)$, is proportional to the regular Airy function, as noted in Section 1.1. Since the properties and numerical values of $Ai(a_1)$ are well known [1,39,47], we have neither tabulated nor plotted $O_1(a_1)$ in this paper. The caustic for this case is easily calculated as in Section 3.3.1 to be $a_1 = 0$; the phase has zero and two real critical points for $a_1 > 0$ and $a_1 < 0$ respectively.

However, we do tabulate and plot values for the evenoid of order 1, $E_1(a_1)$. Table 1 gives numerical values for $a_1 = -8.0(2.0)8.0$ and figure 5 is a plot of $|E_1(a_1)|$ for $a_1 = -16.0(0.001)16.0$. Again, the caustic is $a_1 = 0$. When $a_1 > 0$, the phase has one real critical point, whereas for $a_1 < 0$ there are three. The oscillations associated with the three real critical points are clearly visible in figure 5.

a_1	$\Re E_1(a_1)$	$\Im E_1(a_1)$
-8.0	-0.4772053165	-1.2393662938
-6.0	0.2252567447	-2.0978736136
-4.0	-0.9157889679	-0.8621339148
-2.0	3.3738274073	-1.5351408559
0.0	2.3685438156	0.9810829715
2.0	1.3067746514	1.0309715544
4.0	0.9149664373	0.8396116740
6.0	0.7365902279	0.7071827067
8.0	0.6334482647	0.6188848076

Table 1
Numerical values of $E_1(a_1)$ for the grid $a_1 = -8.0(2.0)8.0$

Table 2 reports numerical values for $O_2(a_1, a_2)$ on the grid $a_1 = -3.0(1.5)3.0$ and $a_2 = -3.0(1.5)3.0$. We show in figure 6 a perspective plot of $O_2(a_1, a_2)$ using the grid $a_1 = -9.0(0.09)9.0$ and $a_2 = -9.0(0.09)9.0$ (i.e. 40401 evaluations of $O_2(a_1, a_2)$), together with the caustic $\{a_1 = 0\} \cup \{(z^2, -2z) : z \geq 0\}$, derived in Section 3.3.2.

a_1	a_2	$O_2(a_1, a_2)$	a_1	a_2	$O_2(a_1, a_2)$
-3.0	-3.0	1.1559094739	0.0	1.5	1.8257400430
-3.0	-1.5	-0.9343849134	0.0	3.0	1.5225522111
-3.0	0.0	-1.0652024273	1.5	-3.0	3.0388228258
-3.0	1.5	0.1821321070	1.5	-1.5	1.0467343593
-3.0	3.0	0.9163784304	1.5	0.0	0.6730914803
-1.5	-3.0	-0.4054310830	1.5	1.5	0.6214013026
-1.5	-1.5	0.4873744213	1.5	3.0	0.6062151325
-1.5	0.0	2.1321475334	3.0	-3.0	-0.9795776028
-1.5	1.5	2.2966206454	3.0	-1.5	-0.3557810576
-1.5	3.0	2.1167618309	3.0	0.0	-0.0385774942
0.0	-3.0	2.0391008331	3.0	1.5	0.0839471717
0.0	-1.5	3.3406774822	3.0	3.0	0.1455363124
0.0	0.0	2.4096436732			

Table 2
Numerical values of $O_2(a_1, a_2)$ for the grid $a_1 = -3.0(1.5)3.0$ and $a_2 = -3.0(1.5)3.0$

The corresponding numerical values for the evenoid of order 2, $E_2(a_1, a_2)$, are given in Table 3 for the grid $a_1 = -4.0(2.0)4.0$ and $a_2 = -4.0(2.0)4.0$. Figure 7 displays a perspective plot of $|E_2(a_1, a_2)|$ for the grid $a_1 = -12.0(0.08)12.0$ and $a_2 = 12.0(0.08)12.0$ (90601 evaluations) together with the caustic $\{a_1 = 0\} \cup \{(z^2, -2z) : z \geq 0\}$, which is the same as for $O_2(a_1, a_2)$.

There are 0,2,4 real critical points for $O_2(a_1, a_2)$ and 1,3,5 for $E_2(a_1, a_2)$. It can be seen that the caustics, together with the number of real critical points in different regions, help rationalise structure in the plots of $O_2(a_1, a_2)$ and $|E_2(a_1, a_2)|$ in figures 6 and 7 respectively.

a_1	a_2	$\Re E_2(a_1,a_2)$	$\Im E_2(a_1,a_2)$	a_1	a_2	$\Re E_2(a_1,a_2)$	$\Im E_2(a_1,a_2)$
-4.0	-4.0	1.3658400830	-1.2384695106	0.0	2.0	1.8879693402	0.6820688232
-4.0	-2.0	1.3579693482	0.0065532688	0.0	4.0	1.6425811883	0.6365965993
-4.0	0.0	0.5952741551	-2.0546457301	2.0	-4.0	3.3150050431	-1.0100166343
-4.0	2.0	2.0646075621	-1.5702447482	2.0	-2.0	2.0502198134	1.4809718645
-4.0	4.0	2.2462420225	-0.8292269526	2.0	0.0	1.4504429717	1.0400416223
-2.0	-4.0	0.6005254417	-1.2809521071	2.0	2.0	1.2981344718	0.8497648666
-2.0	-2.0	0.5584004295	-1.8616971086	2.0	4.0	1.2156705868	0.7503969035
-2.0	0.0	2.7376871800	-1.0988017846	4.0	-4.0	1.6631590653	2.6192314545
-2.0	2.0	2.4754389350	-0.1373334847	4.0	-2.0	0.8838268961	1.1412120618
-2.0	4.0	2.1289408597	0.1604374957	4.0	0.0	0.9459845200	0.8891553653
0.0	-4.0	1.5024596090	0.0778134359	4.0	2.0	0.9461574187	0.7847193584
0.0	-2.0	3.3715185925	-0.6021984749	4.0	4.0	0.9341284566	0.7198386013
0.0	0.0	2.4159183706	0.6473433764				

Table 3
Numerical values of $E_2(a_1, a_2)$ for the grid $a_1 = -4.0(2.0)4.0$ and $a_2 = -4.0(2.0)4.0$

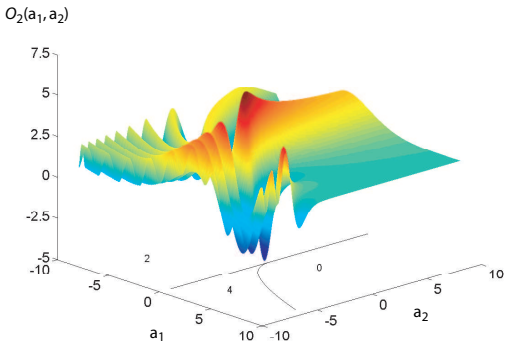

Fig. 6. Plot of $O_2(a_1, a_2)$ for the grid $a_1 = -9.0(0.09)9.0$ and $a_2 = -9.0(0.09)9.0$

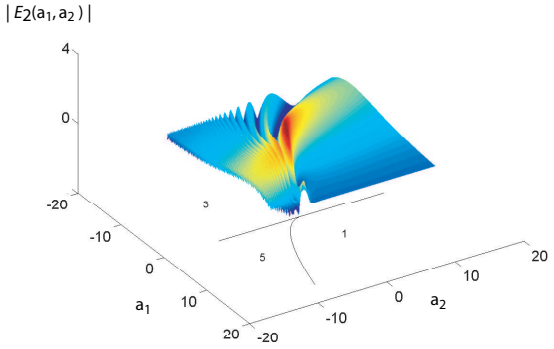

Fig. 7. Plot of $|E_2(a_1, a_2)|$ for the grid $a_1 = -12.0(0.08)12.0$ and $a_2 = -12.0(0.08)12.0$

4.3 Oddenoids of order $k = 3$

Table 4 gives numerical values of $O_3(a_1, a_2, a_3)$ for the grid $a_1, a_2, a_3 = -4.5(4.5)4.5$ whilst numerical values of $E_3(a_1, a_2, a_3)$ are reported in Table 5 using the grid

$a_1, a_2, a_3 = -6.0(6.0)6.0.$

a_1	a_2	a_3	$O_3(a_1, a_2, a_3)$	a_1	a_2	a_3	$O_3(a_1, a_2, a_3)$
-4.5	-4.5	-4.5	0.3860302679	0.0	0.0	4.5	1.7492490911
-4.5	-4.5	0.0	-0.5046555196	0.0	4.5	-4.5	3.2092929414
-4.5	-4.5	4.5	-0.2104031324	0.0	4.5	0.0	1.3805444446
-4.5	0.0	-4.5	0.2059135346	0.0	4.5	4.5	1.2921683755
-4.5	0.0	0.0	-0.6372347560	4.5	-4.5	-4.5	-0.5316027476
-4.5	0.0	4.5	-0.9389067251	4.5	-4.5	0.0	-1.2701643505
-4.5	4.5	-4.5	0.2833242548	4.5	-4.5	4.5	-0.3162980311
-4.5	4.5	0.0	-0.6957156566	4.5	0.0	-4.5	-0.8647916533
-4.5	4.5	4.5	-0.1231373375	4.5	0.0	0.0	-0.0705415393
0.0	-4.5	-4.5	1.2679160361	4.5	0.0	4.5	-0.0504028522
0.0	-4.5	0.0	1.1302960423	4.5	4.5	-4.5	0.2687232428
0.0	-4.5	4.5	2.3788684059	4.5	4.5	0.0	0.0373000249
0.0	0.0	-4.5	1.4432320387	4.5	4.5	4.5	0.0413759219
0.0	0.0	0.0	2.4084941551				

Table 4
Numerical values of $O_3(a_1, a_2, a_3)$ for the grid $a_1, a_2, a_3 = -4.5(4.5)4.5$

a_1	a_2	a_3	$\Re E_3(a_1, a_2, a_3)$	$\Im E_3(a_1, a_2, a_3)$	a_1	a_2	a_3	$\Re E_3(a_1, a_2, a_3)$	$\Im E_3(a_1, a_2, a_3)$
-6.0	-6.0	-6.0	0.7634181196	-0.4343058249	0.0	0.0	6.0	1.7673843126	0.4577842698
-6.0	-6.0	0.0	1.0614215317	-0.2464295636	0.0	6.0	-6.0	2.3867149447	0.3025395109
-6.0	-6.0	6.0	0.0082292456	-0.6943656155	0.0	6.0	0.0	1.5190997036	0.6003264757
-6.0	0.0	-6.0	0.6335885704	-0.8703799424	0.0	6.0	6.0	1.4219788305	0.4994023971
-6.0	0.0	0.0	-0.0911980182	-0.6511890094	6.0	-6.0	-6.0	1.8811081228	0.7194017881
-6.0	0.0	6.0	1.2210838619	-1.4833483531	6.0	-6.0	0.0	0.8330545013	2.0091790377
-6.0	6.0	-6.0	0.7841550140	-0.6173295141	6.0	-6.0	6.0	0.8525566347	0.9294718703
-6.0	6.0	0.0	1.7251591431	-1.3612958534	6.0	0.0	-6.0	0.8453315601	1.9060732990
-6.0	6.0	6.0	1.7517659030	-0.8295259038	6.0	0.0	0.0	0.7240301468	0.7485154536
0.0	-6.0	-6.0	1.2573310357	-0.5959605832	6.0	0.0	6.0	0.8025007257	0.7076430337
0.0	-6.0	0.0	0.9350178145	-0.3371821981	6.0	6.0	-6.0	1.2909570698	-0.6984656479
0.0	-6.0	6.0	2.3481694461	-0.1370488621	6.0	6.0	0.0	0.7589038781	0.6310674245
0.0	0.0	-6.0	1.5826672465	-0.5591557707	6.0	6.0	6.0	0.7794286795	0.6123795565
0.0	0.0	0.0	2.3956449085	0.4765234002					

Table 5
Numerical values of $E_3(a_1, a_2, a_3)$ for the grid $a_1, a_2, a_3 = -6.0(6.0)6.0$

From Section 3.3.3 we know that the caustic for $k = 3$ is the surface described parametrically by equation (59). We have taken sections through this surface for $a_3 = 5$, $a_3 = 0$ and $a_3 = -5$. Perspective plots of $O_3(a_1, a_2, a_3)$ at these three values of a_3 are shown in figures 8, 9, 10 respectively, where the grids used in each case are $a_1 = -21.0(0.09)20.94$ and $a_2 = -21.0(0.09)20.94$ (making 218089 calculations for each plot). The number of real critical points in figures

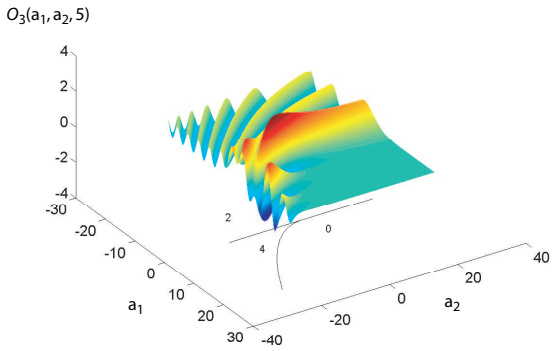

Fig. 8. Plot of $O_3(a_1, a_2, 5)$ for the grid $a_1 = -21.0(0.09)21.94$ and $a_2 = -21.0(0.09)21.94$

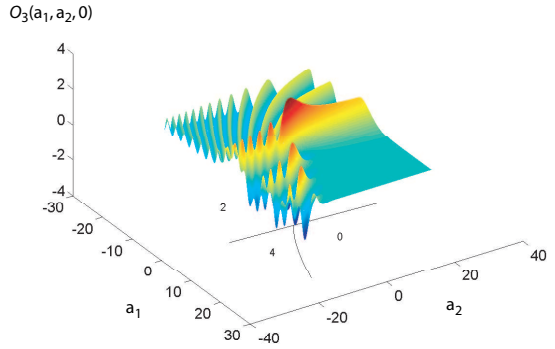

Fig. 9. Plot of $O_3(a_1, a_2, 0)$ for the grid $a_1 = -21.0(0.09)21.94$ and $a_2 = -21.0(0.09)21.94$

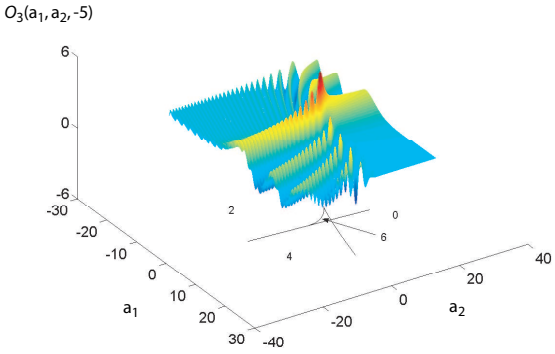

Fig. 10. Plot of $O_3(a_1, a_2, -5)$ for the grid $a_1 = -21.0(0.09)21.94$ and $a_2 = -21.0(0.09)21.94$

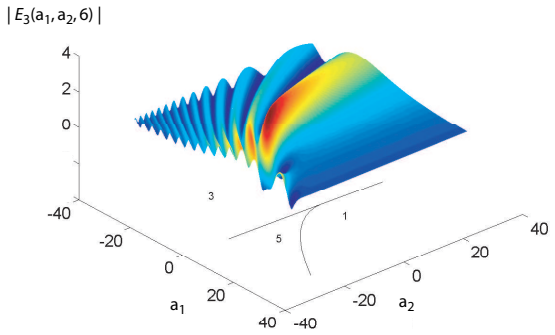

Fig. 11. Plot of $|E_3(a_1, a_2, 6)|$ for the grid $a_1 = -24.0(0.08)24.0$ and $a_2 = -24.0(0.08)24.0$

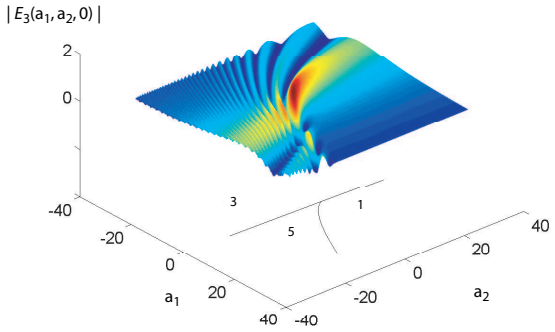

Fig. 12. Plot of $|E_3(a_1, a_2, 0)|$ for the grid $a_1 = -24.0(0.08)24.0$ and $a_2 = -24.0(0.08)24.0$

8 – 10 are 0,2,4 or 6. Each caustic section can be seen to provide a "skeleton" on which is built the wave structure of $O_3(a_1, a_2, a_3)$.

Finally, we plot the modulus of the evenoid of order 3, $E_3(a_1, a_2, a_3)$. Again, the caustic is given in parametric form by equation (59), and to illustrate this surface we take sections through it at $a_3 = 6$, $a_3 = 0$ and $a_3 = -6$. Perspective plots of $|E_3(a_1, a_2, a_3)|$ at these three values of a_3 are shown in figures 11, 12, 13 respectively, where the grids used in each case are $a_1 = -24.0(0.08)24.0$ and $a_2 = -24.0(0.08)24.0$ (making 361201 evaluations for each plot). For this example, the number of real critical points is 1,3,5 or 7 and it can be seen that $|E_3(a_1, a_2, a_3)|$ possesses a rich interference structure as its parameters are varied.

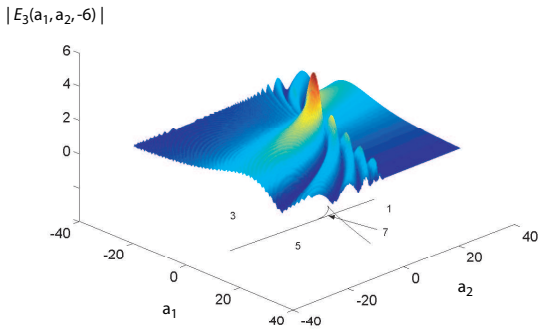

Fig. 13. Plot of $|E_3(a_1, a_2, -6)|$ for the grid $a_1 = -24.0(0.08)24.0$ and $a_2 = -24.0(0.08)24.0$

5 Concluding remarks

We have investigated properties of the oddoids and evenoids that are useful for their numerical evaluation. We studied in detail oddenoids of orders $k = 1, 2, 3$ since it is very difficult to visualise oddenoids with $k > 3$. For each oddenoid, we derived their Maclaurin series representation. For special values of the oddenoid's parameters, we investigated their relation to Airy-Hardy integrals, which allows the oddenoids to be evaluated in terms of Bessel functions of fractional orders. In addition, we obtained the differential equation that $E_1(a_1)$ satisfies, from which we deduced a useful identity obeyed by $E_1(a_1)$ and its first derivative. Singularity theory techniques were used to deduce the caustic, or bifurcation set, associated with the oddenoids. We showed that each oddoid and evenoid of the same order has the same caustic. The bifurcation sets can possess complex whiskers which arise from the coalescence of complex valued critical points. We also presented tables of numerical values and plots of the oddenoids computed using CUSPINT. The rich structure present in the plots was rationalised using the caustics and the number of real critical points in different regions of parameter space.

Finally we note that our investigation can be extended to compute numerical values of the derivatives of the oddenoids, which are required in uniform asymptotic theories of oscillating integrals.

Acknowledgements

Support of this research by the UK Engineering and Physical Sciences Research Council is gratefully acknowledged. We thank the referees for their comments and the Department of Mathematics, University of Bristol, where

this research was completed, for its hospitality.

References

[1] British Association for the Advancement of Science, The Airy Integral Giving Tables of Solutions of the Differential Equation $y'' = xy$, prepared by J. C. P. Miller on behalf of the Committee for the Calculation of Mathematical Tables Part-Volume B (Published for the Royal Society at the Cambridge University Press, Cambridge, 1971).

[2] N. C. Albertsen, P. Balling, N. E. Jensen, Caustics and caustic corrections to the field diffracted by a curved edge. *IEEE Trans. Antennas Prop.* 1977 (25), 297–303.

[3] V. I. Arnold, Arnold's Problems, 2nd edn. (Springer, Berlin, 2005), originally published in Russian as "Zadachi Arnolda" by PHASIS, Moscow, 2000.

[4] M. V. Berry and M. R. Jeffrey, Chiral conical diffraction, J. Opt. A: Pure Appl. Opt., 8 (2006) 363–372.

[5] L. Brillouin, Sur une méthode de calcul approchée de certaines intégrales dite méthode de col, Ann.Sci. École Norm. Sup. Paris, 33 (1916) 17-69.

[6] J. W. Bruce, P. J. Giblin, Curves and Singularities: A Geometrical Introduction to Singularity Theory, 2nd edn. (Cambridge University Press, Cambridge, 1992).

[7] D. Cox, J. Little, D. O'Shea, Ideals, Varieties and Algorithms, 2nd edn. (Springer, New York, 1997).

[8] J. N. L. Connor, P. R. Curtis, R. A. W. Young, Uniform asymptotics of oscillating integrals: applications in chemical physics, in *Wave Aysmptotics, Proceedings of the Meeting to Mark the Retirement of Professor Fritz Ursell from the Beyer Chair of Applied Mathematics in the University of Manchester*, P. A. Martin, G. A. Wickham (Eds), Cambridge University Press, Cambridge, 1972) pp. 24–42.

[9] J. N. L. Connor, Semiclassical theory of molecular collisions: three nearly coincident classical trajectories, Mol. Phys. 26 (1973) 1217–1231.

[10] J. N. L. Connor, Semiclassical theory of molecular collisions: many nearly coincident classical trajectories, Mol. Phys. 27 (1974) 853–866.

[11] J. N. L. Connor, Catastrophes and molecular collisions, Mol. Phys. 31 (1976) 33–55.

[12] J. N. L. Connor, D. Farrelly, Molecular collisions and cusp catastrophes: three methods for the calculation of Pearcey's integral and its derivatives, Chem. Phys. Lett. 81 (1981) 306–310.

[13] J. N. L. Connor, D. Farrelly, Theory of cusped rainbows in elastic scattering: Uniform semiclassical calculations using Pearcey's integral., J. Chem. Phys. 75 (1981) 2831–2846.

[14] J. N. L. Connor, P. R. Curtis, A method for the numerical evaluation of the oscillatory integrals associated with the cuspoid catastrophes: application to Pearcey's integral and its derivatives, J. Phys. A: Math Gen. 15 (1982) 1179–1190.

[15] J. N. L. Connor, P. R. Curtis, D. Farrelly, A differential equation method for the numerical evaluation of the Airy, Pearcey and swallowtail canonical integrals and their derivatives, Mol. Phys. 48 (1983) 1305–1330.

[16] J. N. L. Connor, P. R. Curtis, Differential equations for the cuspoid canonical integrals, J. Math. Phys. 25 (1984) 2895–2902.

[17] J. N. L. Connor, P. R. Curtis, D. Farrelly, The uniform asymptotic swallowtail approximation: practical methods for oscillating integrals with four coalescing saddle points, J. Phys. A: Math. Gen. 17 (1984) 283–310.

[18] J. N. L. Connor, Practical methods for the uniform asymptotic evaluation of oscillating integrals with several coalescing saddle points, in: Asymptotic and Computational Analysis, Conference in Honor of Frank. W.J. Olver's 65th Birthday, R. Wong (Ed.) (Dekker, New York, 1990) pp. 137–173.

[19] J. N. L. Connor, C. A. Hobbs, Numerical evaluation of cuspoid and bessoid oscillating integrals for applications in chemical physics, Khim. Fiz. 23(2) (2004) 13–19. Also available at http://arXiv.org/abs/physics/0411015.

[20] T. Fabčič, J. Main, T. Bartsch, G. Wunner, Photoabsorption spectra of the diagrammatic hydrogen atom in the transition regime to chaos: closed orbit theory with bifurcating orbits, J. Phys. B: At. Mol. Opt. Phys. 38 (2005) S219–S239.

[21] J. Fischer, Über die Beugungserscheinungen bei sphärischer Aberration, Annalen Phys. 72 (1923) 353–399.

[22] A. Gil, J. Segura, N. M. Temme, Computing special functions by using quadrature rules, Numerical Algorithms 33 (2003), 265–275.

[23] M. Golubitsky, D. G. Schaeffer, Singularities and Groups in Bifurcation Theory, Vol. 1 (Springer, New York, 1985).

[24] W. Gröbner, N. Hofreiter, Integraltafel, Zweiter Teil, Bestimmte Integrale, Fünfte, verbesserte Auflage, (Springer-Verlag, Vienna, 1973) section 333, p.118, items (11a) and (11b).

[25] G. H. Hardy, On certain definite integrals considered by Airy and Stokes, Quart. J. 41 (1910) 226–240 [reprinted in: Collected Papers of G. H. Hardy, Vol. 4, edited by a Committee appointed by The London Mathematical Society (Clarendon, Oxford, 1969) pp. 460–474].

[26] D. Kaminski, R. B. Paris, On the zeroes of the Pearcey integral, J. Comput. Appl. Math. 107 (1999) 31–52.

[27] I. Kay and J. B. Keller, Asymptotic evaluation of the field at a caustic. J. Appl. Phys. 25 (1954) 876–883.

[28] Yu. A. Kratsov, Yu. I. Orlov, Caustics, Catastrophes and Wave Fields, 2nd edn. (Springer, Berlin, 1999).

[29] N. P. Kirk, J. N. L. Connor, C. A. Hobbs, An adaptive contour code for the numerical evaluation of the oscillatory cuspoid canonical integrals and their derivatives, Comput. Phys. Commun. 132 (2000) 142–165.

[30] N. P. Kirk, J. N. L. Connor, P. R. Curtis, C. A. Hobbs, Theory of axially symmetric cusped focusing: numerical evaluation of a bessoid integral by an adaptive contour algorithm, J. Phys. A: Math. Gen. 33 (2000) 4797–4808.

[31] J. Kofler, N. Arnold, Axially symmetric focusing of light in dry laser cleaning and nanopatterning, in *Laser Cleaning II*, D. Kane (Ed), World Scientific, Singapore, 2006, in press.

[32] H. Krüger, Semiclassical bound-continuum Franck-Condon factors uniformly valid at 4 coinciding critical points: 2 crossings and 2 turning points, Theoret. Chim. Acta 59 (1981) 97–116.

[33] C. Leubner, Spectral and angular distrbution of synchro-Compton radiation in a linearly polarized vacuum wave of arbitrary intensity, Astron. Astrophys. 96 (1981) 373–379.

[34] C. Leubner, Uniform asymptotic expansion of a class of generalised Bessel functions occurring in the study of fundamental scattering processes in intense laser fields, Phys. Rev. A 23 (1981) 2877–2890.

[35] W. Magnus, F. Oberhettinger, R. P. Soni, Formulas and Theorems for the Special Functions of Mathematical Physics, 3rd enlarged edition (Springer, New York, 1966).

[36] J. Main, Use of harmonic inversion techniques in semiclassical quantization and analysis of quantum spectra, Phys. Rep. 316 (1999) 233–338.

[37] P. L. Marston, Geometrical and catastrophe optics methods in scattering, Phys. Acoustics 21 (1992) 1–234.

[38] J. F. Nye, The relation between the spherical aberration of a lens and the spun cusp diffraction catastrophe, J. Opt. A: Pure Appl. Opt. 7 (2005) 95–102.

[39] F. W. J. Olver, Asympototics and Special Functions (Peters, Wellesley, Massechusetts, 1997).

[40] R. B. Paris D. Kaminski, Asymptotics and Mellin-Barnes Integrals (Cambridge University Press, Cambridge, 2001.)

[41] T. Pearcey, The structure of an electromagnetic field in the neighbourhood of a cusp of a caustic, Phil. Mag. 73 (1946) 311–317.

[42] T. Poston, I. N. Stewart, Taylor Expansions and Catastrophes (Pitman, London, 1976.)

[43] T. Poston and I. Stewart, Catastrophe Theory and Its Applications, An unabridged, unaltered republication of the work first published by Pitman Publishing Limited, London, 1978 in the series "Surveys and Reference Works in Mathematics", (Dover, Mineola, New York, 1996).

[44] J. J. Stamnes, Waves in Focal Regions: Propagation, Diffraction and Focusing of Light, Sound and Water Waves (Hilger, Bristol, 1986).

[45] C. A. Stewart, Advanced Calculus, 3rd ed. (Methuen, London, 1951) section 12.7.

[46] N. M. Temme, Special Functions, An Introduction to the Classical Functions of Mathematical Physics (Wiley, New York, 1996).

[47] O. Vallée, M. Soares, Airy Functions and Applications to Physics (Imperial College Press, London, 2004.)

[48] G. N. Watson, A Treatise on the Theory of Bessel Functions, 2nd edn. (Cambridge University Press, Cambridge, 1966) pp. 320–324.

[49] R. Wong, Asymptotic Approximations of Integrals (SIAM, Philadelphia, 2001).

[50] F. J. Wright, Singularities of plane curves which occur as singular sections of the bifurcation sets of the cuspoid catastrophes, J. Phys. A: Math. Gen. 14 (1981) 1587–1599.

[51] A. E. R. Woodcock, T. Poston, A Geometrical Study of the Elementary Catastrophes, Lect. Notes in Mathematics, No. 373 (Springer-Verlag, Berlin, 1974.)